DOI: 10.1002/ejic.200700092

Conformational Analysis of One-Dimensional Coordination Polymers Based on $[Cp_2Cr_2(CO)_4(\mu,\eta^2\text{-}P_2)]$ by Solid-State Multinuclear NMR Spectroscopy and Density Functional Calculations

Manfred Scheer,*[a] Laurence J. Gregoriades,[a] Manfred Zabel,[a] Marek Sierka,[b] Long Zhang,[c] and Hellmut Eckert*[c]

Dedicated to Professor Joachim Heinicke on the occasion of his 60th birthday

Keywords: Chromium / Copper / Halides / Density functional calculations / NMR spectroscopy / Phosphorus

Reaction of the complex $[Cp_2Cr_2(CO)_4(\mu,\eta^2\text{-}P_2)]$ (**2**) with copper(I) halides leads to the quantitative formation of the new one-dimensional (1D) linear polymers $[CuX\{Cp_2Cr_2(CO)_4(\mu,\eta^2{:}\eta^1{:}\eta^1\text{-}P_2)\}]_n$ [X = Cl (**3**), Br (**4**), I (**5**)]. Polymers **3**–**5** are the first examples of supramolecular aggregates incorporating **2** as a connecting moiety. The solid-state structures of **3**–**5** are compared and their remarkable influence on the respective solid-state ^{31}P magic angle spinning (MAS) NMR spectra is interpreted with the help of density functional theory (DFT) calculations, which suggest that the ^{31}P chemical shifts are extremely sensitive to the position of the phosphorus atoms with respect to the cones of anisotropy of the carbonyl ligands.

(© Wiley-VCH Verlag GmbH & Co. KGaA, 69451 Weinheim, Germany, 2007)

Introduction

The construction of well-defined supramolecular assemblies from discrete units is a field of considerable interest in contemporary chemical research.[1] Typically, different metal centres are connected by suitable N-, O- and/or S-donor-containing organic ligands as linkers. In our research group, however, we utilise organometallic P_n- and As_n-ligand complexes as connecting moieties.[2] The tetrahedrane complex $[Cp_2Mo_2(CO)_4(\mu,\eta^2\text{-}P_2)]$ (**1**),[3] for example, has proven to be a particularly versatile supramolecular building block and forms the basis of several oligomers and one-dimensional (1D) polymers isolated in our group.[2a,2d] In view of the versatility of complex **1** as a linker, we decided to investigate the coordination potential of its chromium analogue $[Cp_2Cr_2(CO)_4(\mu,\eta^2\text{-}P_2)]$ (**2**),[4] particularly due to the fact that it is less stable than **1** and readily undergoes fragmentation reactions,[5] and could thus lead to the formation of novel compounds with unusual P_n-ligand arrangements. We report herein the synthesis, characterisation and solid-state ^{31}P magic angle spinning (MAS) NMR spectral features of the new 1D polymers $[CuX\{Cp_2Cr_2(CO)_4(\mu,\eta^2{:}\eta^1{:}\eta^1\text{-}P_2)\}]_n$ [X = Cl (**3**), Br (**4**), I (**5**)], which are the first examples of supramolecular aggregates containing **2** as a linking unit. The MAS NMR spectra are interpreted with the help of density functional theory (DFT) calculations on the compounds **3**–**5** and the results obtained in a previous ^{31}P MAS NMR study on the analogous 1D polymers $[CuX\{Cp_2Mo_2(CO)_4(\mu,\eta^2{:}\eta^1{:}\eta^1\text{-}P_2)\}]_n$ [X = Cl (**6**), Br (**7**), I (**8**)].[2d]

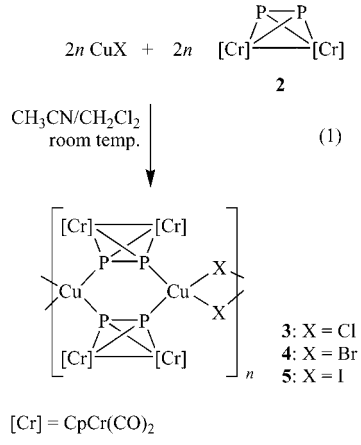

[a] Institut für Anorganische Chemie der Universität Regensburg, 93040 Regensburg, Germany
Fax: +49-941-943-4441
E-mail: mascheer@chemie.uni-regensburg.de
[b] Institut für Chemie der Humboldt-Universität zu Berlin, Unter den Linden 6, 10099 Berlin, Germany
[c] Institut für Physikalische Chemie der Westfälischen Wilhelms-Universität Münster, 48149 Münster, Germany
Fax: +49-251-832-9159
E-mail: eckerth@uni-muenster.de

 © 2007 Wiley-VCH Verlag GmbH & Co. KGaA, Weinheim

Results and Discussion

Synthesis of the Products

Treatment of **2** with CuX (X = Cl, Br, I) in a mixture of CH_3CN and CH_2Cl_2 at room temperature leads to the formation of the 1D polymers **3**–**5** [Equation (1)] as air-sensitive, moss-green microcrystalline powders. The polymers can be stored indefinitely at ambient conditions under an inert atmosphere and are insoluble in most common solvents. They are, however, soluble in trace amounts in polar solvents such as CH_3CN, but then apparently dissociate completely into the starting materials, as evidenced by ^{31}P NMR spectroscopy.

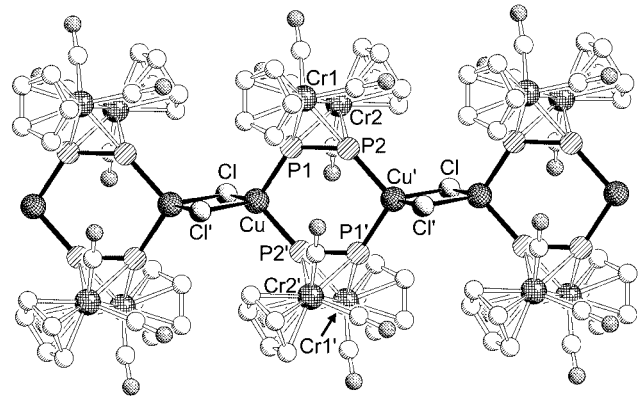

3

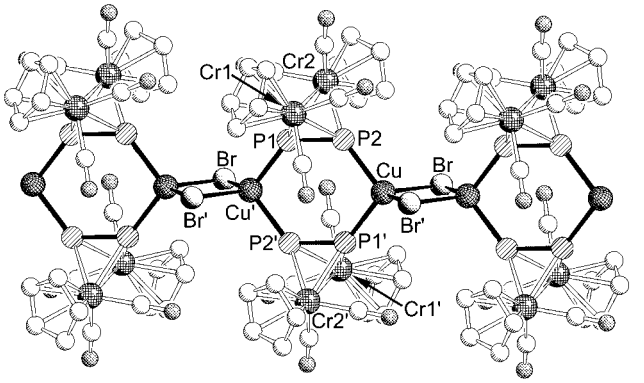

4

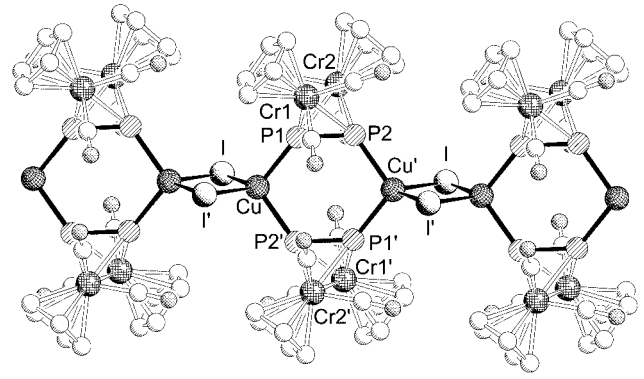

5

Figure 1. Portions of the structures of polymers **3**–**5** (hydrogen atoms have been omitted for clarity). See Table 1 for selected bond lengths and angles.

X-ray Crystallographic Characterisation of the Products

Compounds **3**–**5** were characterised by X-ray crystallography; the measurement details are summarised in the Experimental Section. Their structures display a polymeric core (Figure 1) reminiscent of that in the molybdenum analogues $[CuX\{Cp_2Mo_2(CO)_4(\mu,\eta^2{:}\eta^1{:}\eta^1\text{-}P_2)\}]_n$ [X = Cl (**6**), Br (**7**), I (**8**)].[2a,2d] The Cu^I centres in **3**–**5** are found in a distorted tetrahedral coordination mode and are bridged by the phosphorus atoms of **2** and the halogen atoms. As a result, structures consisting of an alternating arrangement of planar four-membered Cu_2X_2 rings and six-membered Cu_2P_4 rings in a slight chair-like conformation are formed, which are nearly orthogonal to each other. Compounds **4** and **5** and their molybdenum analogues **7** and **8** are structurally similar, whereas polymers **3** and **6** are different. Unlike the molybdenum derivative **6**, the Cu_2P_4 rings in the chromium analogue **3** possess an inversion centre situated at the centre of these rings.

Selected structural details for compounds **3**–**5** are listed in Table 1. The P–P bond lengths of the Cr_2P_2 moieties in **3** and **4** are unchanged compared to uncoordinated **2** [2.060(1) Å],[4a] whereas those in **5** are marginally longer. Although the Cu–P bond lengths are generally longer than those found in complexes of the type $[Cu_2X_2(PPh_3)_3]$[6] (X = Cl:[6a] 2.183(4)–2.245(5) Å; Br:[6b] 2.190(3)–2.260(3) Å; I:[6c] 2.219(3)–2.267(3) Å], the Cu–X bond lengths are within the ranges found in these compounds (X = Cl:[6a] 2.298(4)–2.454(4) Å; Br:[6b] 2.370(2)–2.610(2) Å; I:[6c] 2.500(2)–2.819(1) Å].

Table 1. Comparison of selected bond lengths [Å] and angles [°] in compounds **3**–**5**.

	3 (X = Cl)	**4** (X = Br)	**5** (X = I)
P–P	2.061(1)	2.061(1)	2.073(2)
Cu–P	2.289(1)	2.297(1)	2.323(2)
	2.296(1)	2.305(1)	2.333(2)
Cu–X	2.344(1)	2.467(4)	2.611(1)
	2.363(1)	2.479(4)	2.675(1)
P–Cu–P	103.17(2)	104.07(2)	104.95(7)
P1–Cu–X	111.41(2)	111.97(2)	106.77(6)
	114.53(2)	112.84(2)	116.81(6)
P2–Cu–X	112.02(2)	110.77(2)	106.42(6)
	115.58(2)	113.81(2)	113.17(6)
X–Cu–X	100.49(2)	103.62(2)	108.10(4)
Cu–X–Cu	79.51(2)	76.38(1)	71.90(3)
Cu···Cu···Cu	174.86(1)	176.48(2)	170.50(1)

A further interesting structural feature observed in all three polymers is that the copper atoms are alternately distributed along two parallel lines, as illustrated by the Cu···Cu···Cu angles given in Table 1 and the representation

 © 2007 Wiley-VCH Verlag GmbH & Co. KGaA, Weinheim

of the polymers in Figure 2. Moreover, the folding angle of the Cu_2P_4 rings (dihedral angle between CuP1P2′ and P1P2P1′P2′ planes for **3** and **5**; dihedral angle between CuP1′P2 and P1P2P1′P2′ planes for **4**) decreases as the size of the halogen atom increases (**3**: 3.81(1)°; **4**: 2.48(1)°; **5**: 0.97(1)°].

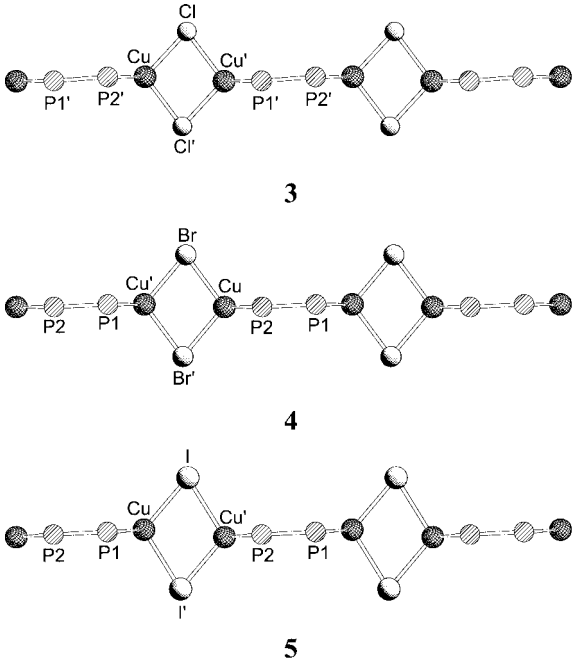

Figure 2. View of the structures of **3**–**5** perpendicular to the faces of the Cu_2X_2 rings, demonstrating that the copper atoms in the polymers are alternately distributed along two parallel lines (chromium atoms and their supporting ligands have been omitted for clarity).

Spectroscopic Characterisation of the Products

Complexes **3**–**5** are soluble in CH_3CN in trace amounts although they apparently dissociate completely into the starting materials according to ^{31}P NMR measurements. However, the fragments detected in the positive-ion ESI mass spectra of the compounds in CH_3CN at room temperature (Table 2) suggest that oligomeric species are most likely also present in solution.

Table 2. Selected fragments [*m*/*z* (relative abundance in %)] detected in the positive-ion ESI mass spectra of compounds **3**–**5** in CH_3CN and the proposed cations for these fragments.

3 (X = Cl)	4 (X = Br)	5 (X = I)	Proposed Cation
1076.7(3)	1166.6(9)	1260.7(12)	$[(Cu_3X_2)\{Cp_2Cr_2(CO)_4P_2\}_2]^+$
1022.6(2)	1110.5(4)	1204.6(7)	$[(Cu_3X_2)\{Cp_2Cr_2(CO)_3P_2\}_2]^+$
978.7(16)	1022.7(18)	1070.6(10)	$[(Cu_2X)\{Cp_2Cr_2(CO)_4P_2\}_2]^+$
922.7(8)	966.6(11)	1014.6(10)	$[(Cu_2X)\{Cp_2Cr_2(CO)_3P_2\}_2]^+$

Solid-state ^{31}P MAS NMR measurements were performed for polymers **3**–**5** at room temperature; the spectra obtained are depicted in Figure 3. The chloride and bromide derivatives exhibit identical spectra and display two multiplets near δ = –100 and 80 ppm, whereas the iodide derivative displays one broad signal at δ = 46.3 ppm with

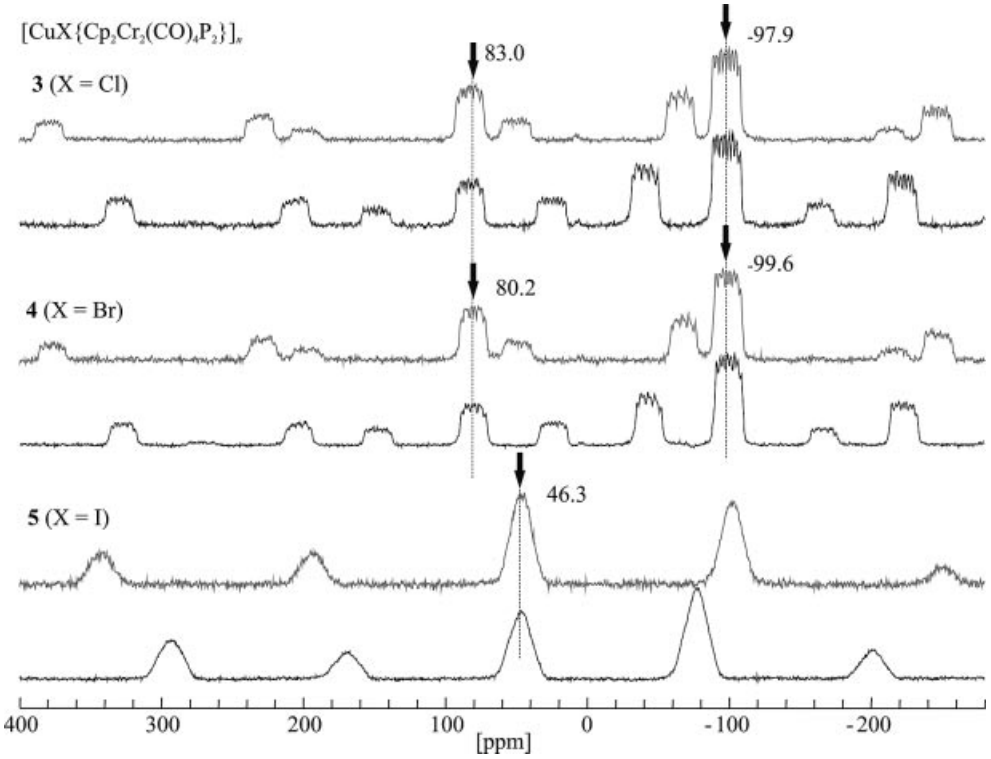

Figure 3. Solid-state ^{31}P MAS NMR spectra of polymers **3**–**5** [X = Cl (**3**), Br (**4**), I (**5**)], recorded with a spinning rate of 25 (bottom) and 30 kHz (top). The peaks marked with arrows are the MAS centre-bands whereas the unmarked peaks are the spinning side-bands.

 © 2007 Wiley-VCH Verlag GmbH & Co. KGaA, Weinheim

no analysable fine structure. These spectra may seem puzzling at first sight considering the solid-state structures of polymers **3**–**5** (Figure 1) as all three polymers contain two sets of crystallographically distinct phosphorus atoms (P1 and P2), which nevertheless appear to be chemically similar. Accordingly, the severely broadened ^{31}P NMR spectrum of the iodide derivative **5** can be interpreted in terms of two unresolved signal components. In contrast, the spectra observed for the chloride and bromide derivatives **3** and **4**, respectively, both of which exhibit two signals separated by about 180 ppm, are initially most surprising. As discussed previously,[2d] we can interpret this observation as a result of the deshielding effect exercised by the cones of anisotropy of the carbonyl ligands. A detailed examination of the structures reveals that the orientation of the P1 and P2 atoms with respect to these ligands differs and, furthermore, the average interatomic distance between the P1 atoms and the carbonyl carbon atoms of the corresponding Cr_2P_2 moieties in **3** and **4** [**3**: 3.128(1) Å; **4**: 3.129(1) Å] is shorter than that of the P2 atoms [**3**: 3.286(1) Å; **4**: 3.279(1) Å]. The corresponding average interatomic distances in **5** are 3.065(1) and 3.079(1) Å. Thus, in analogy to the situation previously described for the molybdenum compounds **6**–**8**,[2d] the environments of the P1 and P2 atoms in **3** and **4** are somewhat different while those of the P1 and P2 atoms in **5** are essentially identical, as suggested by the ^{31}P MAS NMR spectra. While the spectra of **3**–**5** are astonishingly similar to those of the molybdenum analogues **6**–**8**, a satisfactory simulation of the spectrum of **3** (Figure 4) could only be obtained by including the additional effect of $^2J_{P,P}$ coupling; this coupling also manifests itself by broadening effects in the spectrum of **4** (Figure 4).

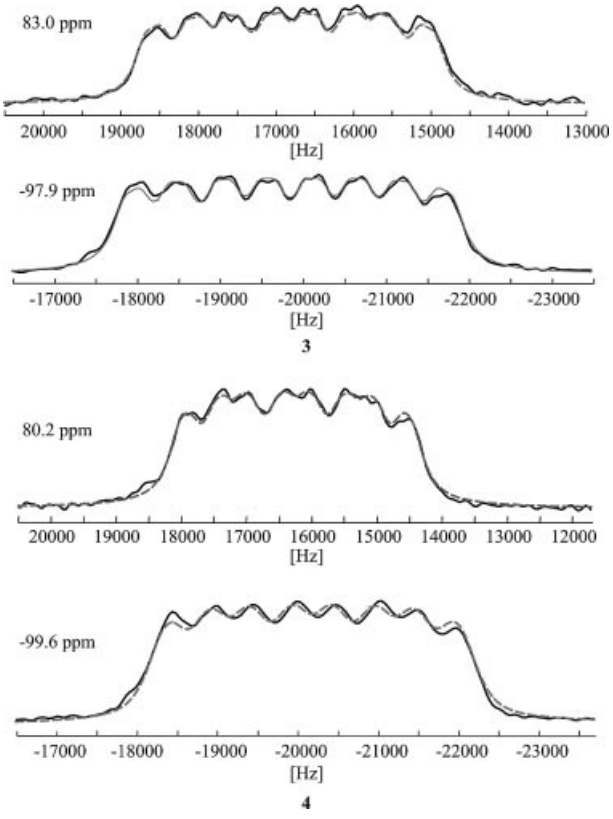

Figure 4. Comparison of the experimental (solid curve) and simulated (dashed curve) solid-state ^{31}P MAS NMR spectra of polymers **3** and **4** (**3**: δ = 83.0 ($^1J_{Cu,P}$ = 1004, $^1J_{P,P}$ = 532, $^2J_{P,P}$ = 200 Hz, P1) and –97.9 ppm ($^1J_{Cu,P}$ = 1079, $^1J_{P,P}$ = 533, $^2J_{P,P}$ = 199 Hz, P2); **4**: δ = 80.2 ($^1J_{Cu,P}$ = 962, $^1J_{P,P}$ = 531, $^2J_{P,P}$ = 195 Hz, P1) and –99.6 ppm ($^1J_{Cu,P}$ = 1024, $^1J_{P,P}$ = 531, $^2J_{P,P}$ = 175 Hz, P2).

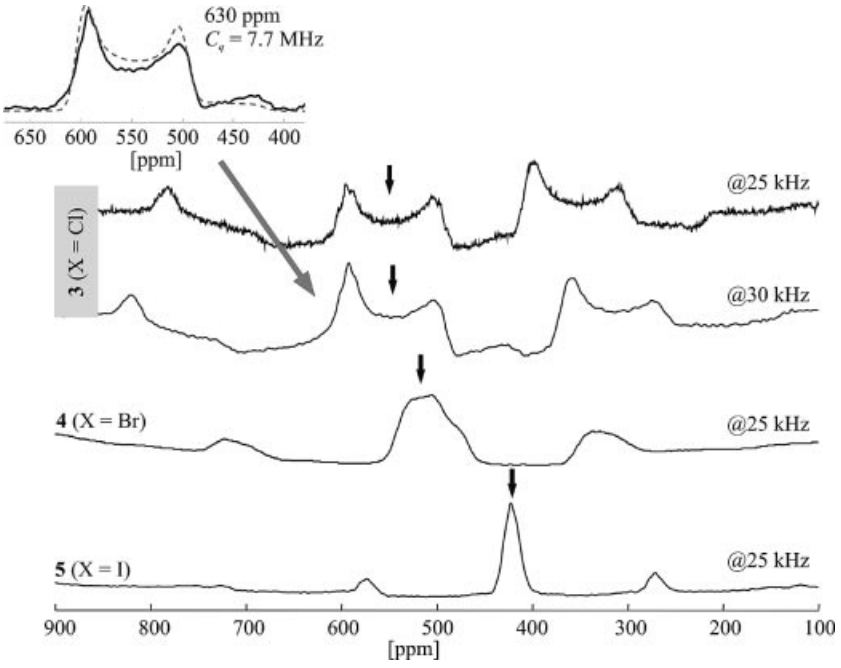

Figure 5. ^{63}Cu MAS NMR spectra of compounds **3** (two different spinning frequencies), **4** and **5**. MAS centre-bands are labelled with black arrows. The inset compares the MAS centre-band (solid curve) to a simulated second-order quadrupolar powder pattern lineshape (dashed curve; η = 0).

 © 2007 Wiley-VCH Verlag GmbH & Co. KGaA, Weinheim

The low-field signals in the spectra of **3** and **4** are assigned to the P1 atoms since they are closer, on average, to the carbonyl ligands than are the P2 atoms, and therefore experience greater deshielding.

The ^{63}Cu MAS NMR spectra of compounds **3**–**5** are presented in Figure 5. The spectrum of **5** exhibits a sharp line centred near δ = 422 ppm vs. crystalline CuI, while the MAS NMR spectra for **3** and **4** are strongly broadened by second-order quadrupolar perturbations. The ^{63}Cu MAS NMR spectrum of **3** could be simulated with an isotropic chemical shift of δ = 630 ppm, a nuclear electric quadrupolar coupling constant of 7.7 MHz and a zero asymmetry parameter by using the dmfit routine. For **4**, the simulation of the experimental spectra yielded an isotropic chemical shift of δ = 550 ppm, and nuclear electric quadrupolar coupling constants of 5.2 and 4.8 MHz for ^{63}Cu and ^{65}Cu, respectively. Since the spectra of **4** were rather poorly resolved, no reliable value could be determined for the asymmetry parameter. The isotropic chemical shifts measured for the copper nuclei within the distorted CuP_2X_2 tetrahedral environments are consistent with those previously measured for the analogous molybdenum-based compounds[2d] and show a monotonic trend along the I → Br → Cl series. Furthermore, inspection of Table 1 reveals that the CuX_2P_2 tetrahedra become increasingly distorted along this series (note the significant trend of the X–Cu–X angles in particular), thereby offering a good structural rationale for the large changes observed in the C_q values measured for the copper nuclei.

Theoretical Calculations

Density functional theory (DFT) calculations were carried out on complexes **3**–**5** to support the ^{31}P MAS NMR assignments proposed above. Full structure optimisations of the crystal structures were performed and the most important calculated structural parameters, which are in very good agreement with the experimental data (Table 1), are presented in Table 3. The calculated ^{31}P NMR chemical shifts (Table 4) are also in very good agreement with the experimental data. For the chloride and bromide derivatives, the calculated chemical shifts of the P1 and P2 atoms are separated by about 200 ppm, whereas in the iodide derivative these shifts differ by 2 ppm. The results of the calculations thus support the deductions inferred.

Table 3. Comparison of selected calculated bond lengths [Å] and angles [°] in compounds **3**–**5**.

	3 (X = Cl)	**4** (X = Br)	**5** (X = I)
P–P	2.075	2.077	2.083
Cu–P	2.252	2.257	2.278
	2.259	2.264	2.280
Cu–X	2.336	2.462	2.615
	2.352	2.472	2.651
P–Cu–P	104.52	105.79	106.79
P1–Cu–X	111.87	112.19	106.89
	115.55	113.84	117.97
P2–Cu–X	112.13	110.72	106.04
	115.24	113.59	113.53
X–Cu–X	97.79	110.85	104.81
Cu–X–Cu	82.21	79.15	75.19
Cu···Cu···Cu	174.90	176.48	169.91

Table 4. Calculated ^{31}P isotropic shielding constants, σ, and chemical shifts, δ [ppm], for compounds **3**–**5**.

	3		**4**		**5**	
	σ	δ	σ	δ	σ	δ
P1	254.2	73.8	252.0	76.0	278.5	49.5
P2	452.8	–124.8	450.8	–122.8	280.6	47.5

Conclusions

The P_2-ligand complex **2** reacts with copper(I) halides to yield the new 1D polymers **3**–**5**. Thus, in contrast to the reactivity of complex **2** towards organometallic Lewis-acidic complexes,[5] the tetrahedrane structure of **2** remains intact upon reaction with copper(I) halides. The cores of **3**–**5** consist of an alternating arrangement of six-membered Cu_2P_4 and four-membered Cu_2X_2 [X = Cl (**3**), Br (**4**), I (**5**)] rings that are nearly orthogonal to each other. This structural motif is reminiscent of that of the 1D polymers **6**–**8**,[2a,2d] which are the molybdenum analogues of compounds **3**–**5**. Polymers **3**–**5** are the first extended assemblies incorporating **2** as a ligand and thus demonstrate the potential of **2** as a supramolecular building block.

Solid-state ^{31}P MAS NMR measurements have been performed on the polymers **3**–**5**. The spectra of **3** and **4** display two well-separated signals, whereas only one broad signal is observed in the spectrum of **5**. Each polymer contains two sets of crystallographically distinct phosphorus atoms (P1 and P2), which, at first sight, appear chemically similar. However, inspection of the average interatomic distances between the phosphorus atoms and the carbonyl carbon atoms of the respective units of **2** has revealed that the P1 and P2 atoms in **3** and **4** are shielded to different degrees by the carbonyl ligands, while the P1 and P2 atoms in **5** are shielded to virtually the same extent. Thus, as already demonstrated for the molybdenum analogues **6**–**8**, the chemical shift of the phosphorus atoms in polymers **3**–**5** appears to be exceedingly sensitive to the position of the phosphorus atoms with respect to the cones of anisotropy of the carbonyl ligands, and this has been confirmed by DFT calculations on these compounds.

Experimental Section

General Remarks: All manipulations were performed under an atmosphere of dry nitrogen using standard glove-box and Schlenk techniques. All solvents were freshly distilled from appropriate drying agents immediately prior to use. IR spectra were recorded with a Varian FTS 2000 spectrometer. Solution NMR spectra were acquired with a Bruker Avance 400 MHz spectrometer. ESI mass spectra were recorded with a Finnigan Thermoquest TSQ 7000 mass spectrometer.

Reagents: $[Cp_2Cr_2(CO)_4(\mu,\eta^2\text{-}P_2)]$ (**2**) was prepared according to the literature procedure.[4b] CuCl (Strem) and CuBr (Strem) were

 © 2007 Wiley-VCH Verlag GmbH & Co. KGaA, Weinheim

purified before use, under a nitrogen atmosphere, by washing with the appropriate aqueous hydrohalic acid (half-concentrated), followed by H_2O, EtOH and Et_2O. The resulting solids were then dried at room temperature under high vacuum and stored in a dry box. CuI (Aldrich) was purified and stored in a similar manner, the only difference being that a mixture of aqueous HCl (half-concentrated) and KI was used as the first washing medium.

Crystal Structure Analysis: Data were collected with a STOE IPDS diffractometer. The structures were solved using SIR-97[7] and refined using SHELXL-97[8] with anisotropic displacements for non-hydrogen atoms. Hydrogen atoms were located in idealised positions and refined isotropically according to the riding model. Further details are given in Table 5.

CCDC-633372 to -633374 (for **3**–**5**, respectively) contain the supplementary crystallographic data for this paper. These data can be obtained free of charge from The Cambridge Crystallographic Data Centre via www.ccdc.cam.ac.uk/data_request/cif.

Solid-State MAS NMR Spectroscopy: ^{31}P, ^{63}Cu and ^{65}Cu MAS NMR spectra were recorded at resonance frequencies of 202.5, 132.6 and 142.1 MHz, respectively, on a Bruker DSX-500 spectrometer equipped with a 2.5-mm NMR probe operating at MAS rotation frequencies of 25–30 kHz. Typical acquisition parameters for single-pulse measurements: pulse length: 3.0 μs (90° flip angle) for ^{31}P and 0.7 μs (30° flip angle) for $^{63,65}Cu$; recycle delay: 150 s for ^{31}P and 1 s for $^{63,65}Cu$; 256–512 scans for ^{31}P and 10000 scans for $^{63,65}Cu$. ^{31}P and $^{63,65}Cu$ NMR chemical shifts are referenced to 85% H_3PO_4 and crystalline CuI, respectively.

Theoretical Calculations: The following procedure was used to calculate the ^{31}P NMR chemical shifts. Starting from the experimental crystal structures, compounds **3**–**5** were fully optimised at the density functional theory (DFT) level using the Vienna Ab initio Simulation Package (VASP)[9,10] along with the Perdew–Wang (PW91)[11] exchange-correlation functional. The electron–ion interactions were described by the projector augmented wave (PAW) method[12] as used by Kresse and Joubert.[13] A plane-wave basis set with an energy cutoff of 300 eV along with appropriate PAW potentials was used. For the integration of the Brillouin zone, a $(1\times2\times1)$ Monkhorst–Pack grid[14] was used for **3** and **4** and a $(2\times1\times1)$ grid for **5**. Next, molecular fragments containing three $[CuX\{Cp_2Cr_2(CO)_4(\mu,\eta^2{:}\eta^1{:}\eta^1\text{-}P_2)\}]$ (X = Cl, Br, I) units terminated with single X atoms were cut out from the optimised structures. The ^{31}P chemical shifts were calculated for the fragments within the GIAO approach,[15] using the BP86 exchange-correlation functional,[16] SVP basis sets[17] and the Gaussian 03 program package.[18] Relativistic effective core potentials were used for iodine.[19] The ^{31}P chemical shifts relative to 85% H_3PO_4 were calculated from absolute shielding constants, σ, by using $PO(CH_3)_3$ as an internal secondary standard (σ = 188.1) with an experimental ^{31}P chemical shift[20] of δ = 140 ppm relative to 85% H_3PO_4.

Synthesis of 3: A solution of CuCl (49 mg, 0.49 mmol) in CH_3CN (10 mL) was carefully layered over a solution of **2** (100 mg, 0.25 mmol) in CH_2Cl_2 (10 mL) at room temperature. The vessel was left at room temperature in the dark and moss-green needles of **3** were deposited within a month. These were filtered, washed with CH_3CN (2×3 mL) and pentane (2×3 mL), in that order, and dried under vacuum. Yield: 100 mg (80%); m.p. 167 °C (decomp.). ^{31}P MAS NMR (202.5 MHz, room temp.): δ = –97.9 (m), 83.0 ppm (m). ^{63}Cu MAS NMR (132.6 MHz, room temp.): δ = 630 ppm (br). Positive-ion ESI MS (CH_3CN, room temp.): *m/z* (%) 1076.7 (3) $[Cu_3Cl_2\{Cp_2Cr_2(CO)_4P_2\}_2]^+$, 1022.6 (2) $[Cu_3Cl_2\{Cp_2Cr_2(CO)_3P_2\}_2]^+$, 978.7 (16) $[Cu_2Cl\{Cp_2Cr_2(CO)_4P_2\}_2]^+$, 922.7 (8) $[Cu_2Cl\{Cp_2Cr_2(CO)_3P_2\}_2]^+$, 878.8 (33) $[Cu\{Cp_2Cr_2(CO)_4P_2\}_2]^+$, 864.7 (2) $[Cu_2Cl\{Cp_2Cr_2(CO)_2P_2\}_2]^+$, 822.8 (43) $[Cu\{Cp_2Cr_2(CO)_3P_2\}_2]^+$, 794.8 (1) $[Cu\{Cp_2Cr_2(CO)_{2.5}P_2\}_2]^+$, 766.8 (22) $[Cu\{Cp_2Cr_2(CO)_2P_2\}_2]^+$, 712.7 (1) $[Cu\{Cp_2Cr_2(CO)P_2\}_2]^+$, 751.8 (1) $[Cu_2Cl\{Cp_2Cr_2(CO)P_2\}_2]^+$, 695.9 (1) $[Cu_2Cl\{Cp_2Cr_2P_2\}_2]^+$, 654.7 (1) $[Cu\{Cp_2Cr_2P_2\}_2]^+$, 511.8 (60) $[Cu\{Cp_2Cr_2(CO)_4P_2\}(NCCH_3)]^+$,

Table 5. Crystallographic data for **3**–**5**.

	3	**4**	**5**·*n*CH_3CN
Empirical formula	$C_{14}H_{10}ClCr_2CuO_4P_2$	$C_{14}H_{10}BrCr_2CuO_4P_2$	$C_{16}H_{13}Cr_2CuINO_4P_2$
M_r	507.16	551.61	639.66
Crystal size [mm]	$0.40\times0.10\times0.06$	$0.46\times0.08\times0.04$	$0.30\times0.06\times0.04$
T [K]	173(1)	173(1)	173(1)
λ [Å]	0.71073	0.71073	0.71073
Crystal system	monoclinic	monoclinic	triclinic
Space group	$P2_1/n$	$P2_1/n$	$P\bar{1}$
a [Å]	14.616(2)	14.614(1)	7.980(1)
b [Å]	7.909(1)	7.943(1)	11.485(1)
c [Å]	16.032(2)	16.120(2)	11.519(1)
α [°]	90	90	82.06(1)
β [°]	112.10(1)	111.72(1)	81.06(1)
γ [°]	90	90	76.85(1)
V [Å^3]	1717.0(3)	1738.4(3)	1009.7(2)
Z	4	4	2
$\rho_{calcd.}$ [g cm^{-3}]	1.962	2.108	2.104
μ [mm^{-1}]	2.827	4.937	3.809
θ range [°]	2.98–25.86	2.90–25.85	1.80–25.90
Reflections collected/unique	23308/3303	14195/3347	6689/3006
Observed reflections with [$I > 2\sigma(I)$]	2852	2692	2225
R_{int}	0.0267	0.0260	0.0998
GOF on F^2	0.997	0.927	0.935
Final R indices [$I > 2\sigma(I)$]	R_1 = 0.0192	R_1 = 0.0203	R_1 = 0.0452
	wR_2 = 0.0501	wR_2 = 0.0475	wR_2 = 0.1070
R indices (all data)	R_1 = 0.0237	R_1 = 0.0281	R_1 = 0.0614
	wR_2 = 0.0513	wR_2 = 0.0491	wR_2 = 0.1122
Max./min. $\Delta\rho$ [e Å^{-3}]	0.343/–0.234	0.538/–0.275	0.979/–0.673

 © 2007 Wiley-VCH Verlag GmbH & Co. KGaA, Weinheim

496.9 (2) $[Cu\{Cp_2Cr_2(CO)_2P_2\}(NCCH_3)_2]^+$, 471.6 (1) $[Cu\{Cp_2Cr_2(CO)_4P_2\}]^+$, 455.8 (100) $[Cu\{Cp_2Cr_2(CO)_2P_2\}(NCCH_3)]^+$, 442.9 (9) $[Cu\{Cp_2Cr_2P_2\}(NCCH_3)_2]^+$ or $[Cu\{Cp_2Cr_2(CO)_3P_2\}]^+$, 427.8 (17) $[Cu\{Cp_2Cr_2(CO)P_2\}(NCCH_3)]^+$. IR (KBr): $\tilde{\nu}$ = 3118 (w), 1993 (vs; CO), 1951 (vs; CO), 1914 (vs; CO), 1880 (vs; CO), 1851 (s; CO), 1424 (m), 1363 (w), 1264 (w), 1116 (w), 1062 (m), 1013 (m), 957 (w), 932 (w), 886 (m), 867 (m), 854 (s), 846 (s), 669 (w), 621 (m), 603 (m), 596 (m), 560 (s), 551 (s), 523 (m), 506 (m), 489 (m), 479 (m), 446 (w), 427 cm^{-1} (w). $C_{14}H_{10}ClCr_2CuO_4P_2$ (507.17): calcd. C 33.16, H 1.99; found C 32.83, H 1.99.

Synthesis of 4: A solution of CuBr (70 mg, 0.49 mmol) in CH_3CN (10 mL) was carefully layered over a solution of **2** (100 mg, 0.25 mmol) in CH_2Cl_2 (10 mL) at room temperature. The vessel was left at room temperature in the dark and moss-green needles of **4** were deposited within a month. These were filtered, washed with CH_3CN (2 × 3 mL) and pentane (2 × 3 mL), in that order, and dried under vacuum. Yield: 120 mg (89%); m.p. 202 °C (decomp.). ^{31}P MAS NMR (202.5 MHz, room temp.): δ = –99.6 (m), 80.2 ppm (m). ^{63}Cu MAS NMR (132.6 MHz, room temp.): δ = 550 ppm (br). Positive-ion ESI MS (CH_3CN, room temp.): *m*/*z* (%) 1166.6 (9) $[Cu_3Br_2\{Cp_2Cr_2(CO)_4P_2\}_2]^+$, 1110.5 (4) $[Cu_3Br_2\{Cp_2Cr_2(CO)_3P_2\}_2]^+$, 1022.7 (18) $[Cu_2Br\{Cp_2Cr_2(CO)_4P_2\}_2]^+$, 1007.6 (2) $[Cu_2Br\{Cp_2Cr_2(CO)_3P_2\}_2(NCCH_3)]^+$, 966.6 (11) $[Cu_2Br\{Cp_2Cr_2(CO)_3P_2\}_2]^+$, 910.6 (1) $[Cu_2Br\{Cp_2Cr_2(CO)_2P_2\}_2]^+$, 878.8 (40) $[Cu\{Cp_2Cr_2(CO)_4P_2\}_2]^+$, 822.8 (17) $[Cu\{Cp_2Cr_2(CO)_3P_2\}_2]^+$, 799.5 (1) $[Cu_2Br\{Cp_2Cr_2(CO)P_2\}_2]^+$, 766.8 (6) $[Cu\{Cp_2Cr_2(CO)_2P_2\}_2]^+$, 743.6 (1) $[Cu_2Br\{Cp_2Cr_2P_2\}_2]^+$, 655.7 (2) $[Cu\{Cp_2Cr_2P_2\}_2]^+$, 599.8 (5) $[Cu_2Br\{Cp_2Cr_2(CO)_2P_2\}(NCCH_3)]^+$, 511.8 (100) $[Cu\{Cp_2Cr_2(CO)_4P_2\}(NCCH_3)]^+$, 496.8 (8) $[Cu\{Cp_2Cr_2(CO)_2P_2\}(NCCH_3)_2]^+$, 468.9 (2) $[Cu\{Cp_2Cr_2(CO)_4P_2\}]^+$, 455.8 (45) $[Cu\{Cp_2Cr_2(CO)_2P_2\}(NCCH_3)]^+$, 440.8 (9) $[Cu\{Cp_2Cr_2P_2\}(NCCH_3)_2]^+$ or $[Cu\{Cp_2Cr_2(CO)_3P_2\}]^+$, 427.8 (5) $[Cu\{Cp_2Cr_2(CO)P_2\}(NCCH_3)]^+$. IR (KBr): $\tilde{\nu}$ = 3113 (w), 1995 (vs; CO), 1951 (vs; CO), 1915 (vs; CO), 1881 (vs; CO), 1851 (s; CO), 1424 (m), 1363 (w), 1265 (w), 1116 (w), 1060 (w), 1005 (w), 956 (w), 930 (w), 886 (w), 867 (m), 852 (s), 669 (w), 620 (m), 602 (m), 596 (m), 559 (s), 550 (s), 521 (m), 504 (m), 488 (m), 478 (s), 445 cm^{-1} (w). $C_{14}H_{10}BrCr_2CuO_4P_2$ (551.62): calcd. C 30.48, H 1.83; found C 30.13, H 1.81.

Synthesis of 5·*n*CH_3CN: A solution of CuI (93 mg, 0.49 mmol) in CH_3CN (10 mL) was carefully layered over a solution of **2** (100 mg, 0.25 mmol) in CH_2Cl_2 (10 mL) at room temperature. The vessel was left at room temperature in the dark and moss-green needles of **5**·*n*CH_3CN were deposited within a month. These were filtered, washed with CH_3CN (2 × 3 mL) and pentane (2 × 3 mL), in that order, and dried under vacuum at room temperature. The solvent of crystallisation was not lost during the drying process. Yield: 140 mg (89%); m.p. 184 °C (decomp.). ^{31}P MAS NMR (202.5 MHz, room temp.): δ = 46.3 ppm (br). ^{63}Cu MAS NMR (132.6 MHz, room temp.): δ = 422 (br). Positive-ion ESI MS (CH_3CN, room temp.): *m*/*z* (%) 1260.7 (12) $[Cu_3I_2\{Cp_2Cr_2(CO)_4P_2\}_2]^+$, 1204.6 (7) $[Cu_3I_2\{Cp_2Cr_2(CO)_3P_2\}_2]^+$, 1070.6 (10) $[Cu_2I\{Cp_2Cr_2(CO)_4P_2\}_2]^+$, 1055.6 (1) $[Cu_2I\{Cp_2Cr_2(CO)_3P_2\}_2(NCCH_3)]^+$, 1014.6 (11) $[Cu_2I\{Cp_2Cr_2(CO)_3P_2\}_2]^+$, 958.6 (2) $[Cu_2I\{Cp_2Cr_2(CO)_2P_2\}_2]^+$, 878.8 (35) $[Cu\{Cp_2Cr_2(CO)_4P_2\}_2]^+$, 822.8 (17) $[Cu\{Cp_2Cr_2(CO)_3P_2\}_2]^+$, 766.7 (5) $[Cu\{Cp_2Cr_2(CO)_2P_2\}_2]^+$, 647.7 (4) $[Cu_2I\{Cp_2Cr_2(CO)_2P_2\}(NCCH_3)]^+$, 511.8 (100) $[Cu\{Cp_2Cr_2(CO)_4P_2\}(NCCH_3)]^+$, 496.8 (8) $[Cu\{Cp_2Cr_2(CO)_2P_2\}(NCCH_3)_2]^+$, 468.9 (2) $[Cu\{Cp_2Cr_2(CO)_4P_2\}]^+$, 455.8 (42) $[Cu\{Cp_2Cr_2(CO)_2P_2\}(NCCH_3)]^+$, 440.8 (8) $[Cu\{Cp_2Cr_2P_2\}(NCCH_3)_2]^+$ or $[Cu\{Cp_2Cr_2(CO)_3P_2\}]^+$, 427.8 (6) $[Cu\{Cp_2Cr_2(CO)P_2\}(NCCH_3)]^+$. IR (KBr): $\tilde{\nu}$ = 3123 (w), 3099 (w), 2254 (w; CN), 1992 (vs; CO), 1975 (vs; CO), 1918 (vs; CO), 1425 (m), 1363 (w), 1264 (w), 1116 (w), 1064 (m), 1016 (w), 927 (w), 843 (m), 833 (m), 606 (m), 599 (m), 563 (s), 540 (m), 490 (m), 425 cm^{-1} (w). $C_{16}H_{13}Cr_2CuINO_4P_2$ (639.67): calcd. C 30.04, H 2.05, N 2.19; found C 29.61, H 2.05, N 2.08.

Acknowledgments

This work was supported by the Deutsche Forschungsgemeinschaft and the Fonds der Chemischen Industrie. The authors would like to thank Prof. Joachim Sauer and the Humboldt University of Berlin for providing computing facilities, and Mrs. Petra Lugauer and Mrs. Sabine Stempfhuber for technical assistance.

[1] Recent review articles: a) W. Huang, H.-B. Zhu, S.-H. Gou, *Coord. Chem. Rev.* **2006**, *250*, 414–423; b) N. C. Gianneschi, M. S. Masar III, C. A. Mirkin, *Acc. Chem. Res.* **2005**, *38*, 825–837; c) M. Ruben, J. Rojo, F. J. Romero-Salguero, L. H. Uppadine, J.-M. Lehn, *Angew. Chem.* **2004**, *116*, 3728–3747; *Angew. Chem. Int. Ed.* **2004**, *43*, 3644–3662; d) L. Carlucci, G. Ciani, D. M. Proserpio, *Coord. Chem. Rev.* **2003**, *246*, 247–289; e) G. F. Swiegers, T. J. Malefetse, *Coord. Chem. Rev.* **2002**, *225*, 91–121.

[2] a) J. Bai, E. Leiner, M. Scheer, *Angew. Chem.* **2002**, *114*, 820–823; *Angew. Chem. Int. Ed.* **2002**, *41*, 783–786; b) J. Bai, A. V. Virovets, M. Scheer, *Angew. Chem.* **2002**, *114*, 1808–1811; *Angew. Chem. Int. Ed.* **2002**, *41*, 1737–1740; c) J. Bai, A. V. Virovets, M. Scheer, *Science* **2003**, *300*, 781–783; d) M. Scheer, L. Gregoriades, J. Bai, M. Sierka, G. Brunklaus, H. Eckert, *Chem. Eur. J.* **2005**, *11*, 2163–2169; e) M. Scheer, J. Bai, B. P. Johnson, R. Merkle, A. V. Virovets, C. E. Anson, *Eur. J. Inorg. Chem.* **2005**, 4023–4026; f) B. P. Johnson, F. Dielmann, G. Balázs, M. Sierka, M. Scheer, *Angew. Chem.* **2006**, *118*, 2533–2536; *Angew. Chem. Int. Ed.* **2006**, *45*, 2473–2475; g) L. J. Gregoriades, H. Krauss, J. Wachter, A. V. Virovets, M. Sierka, M. Scheer, *Angew. Chem.* **2006**, *118*, 4295–4298; *Angew. Chem. Int. Ed.* **2006**, *45*, 4189–4192; h) M. Scheer, L. J. Gregoriades, A. V. Virovets, W. Kunz, R. Neueder, I. Krossing, *Angew. Chem.* **2006**, *118*, 5818–5822; *Angew. Chem. Int. Ed.* **2006**, *45*, 5689–5693.

[3] a) O. J. Scherer, H. Sitzmann, G. Wolmershäuser, *J. Organomet. Chem.* **1984**, *268*, C9–C12; b) O. J. Scherer, J. Schwalb, H. Sitzmann, *Inorg. Synth.* **1990**, *27*, 224–227.

[4] a) L. Y. Goh, C. K. Chu, R. C. S. Wong, T. W. Hambley, *J. Chem. Soc., Dalton Trans.* **1989**, 1951–1956; b) L. Y. Goh, R. C. S. Wong, *Inorg. Synth.* **1992**, *29*, 247–250.

[5] a) P. Sekar, M. Scheer, A. Voigt, R. Kirmse, *Organometallics* **1999**, *18*, 2833–2837; b) P. Sekar, S. Umbarkar, M. Scheer, A. Voigt, R. Kirmse, *Eur. J. Inorg. Chem.* **2000**, 2585–2589.

[6] a) V. G. Albano, P. L. Bellon, G. Ciani, M. Manassero, *J. Chem. Soc., Dalton Trans.* **1972**, 171–175; b) H. Negita, M. Hiura, Y. Kushi, M. Kuramoto, T. Okuda, *Bull. Chem. Soc. Jpn.* **1981**, *54*, 1247–1248; c) P. G. Eller, G. J. Kubas, R. R. Ryan, *Inorg. Chem.* **1977**, *16*, 2454–2462. The relatively wide ranges quoted for the Cu–P and Cu–X bond lengths are due to the fact that the Cu atoms in the complexes $[Cu_2X_2(PPh_3)_3]$ are found in both trigonal and tetrahedral coordination modes.

[7] A. Altomare, G. Cascarano, C. Giacovazzo, A. Guagliardi, *J. Appl. Crystallogr.* **1993**, *26*, 343–350.

[8] G. M. Sheldrick, *SHELXL-97*, University of Göttingen, Germany, **1997**.

[9] G. Kresse, J. Furthmüller, *Comput. Mater. Sci.* **1996**, *6*, 15.

[10] G. Kresse, J. Furthmüller, *Phys. Rev. B* **1996**, *54*, 11169.

[11] J. P. Perdew, J. A. Chevary, S. H. Vosko, K. A. Jackson, M. R. Pederson, D. J. Singh, C. Fiolhais, *Phys. Rev. B* **1992**, *46*, 6671.

[12] P. E. Blöchl, *Phys. Rev. B* **1994**, *50*, 17953.

[13] G. Kresse, D. Joubert, *Phys. Rev. B* **1999**, *59*, 1758.

[14] H. J. Monkhorst, J. D. Pack, *Phys. Rev. B* **1976**, *13*, 5188.

[15] G. Schreckenbach, T. Ziegler, *J. Phys. Chem.* **1995**, *99*, 606–611.

[16] a) A. D. Becke, *Phys. Rev. A* **1988**, *38*, 3098–3100; b) S. H. Vosko, L. Wilk, M. Nusair, *Can. J. Phys.* **1980**, *58*, 1200–1211; c)

 © 2007 Wiley-VCH Verlag GmbH & Co. KGaA, Weinheim

J. P. Perdew, *Phys. Rev. B* **1986**, *33*, 8822–8824; erratum: J. P. Perdew, *Phys. Rev. B* **1986**, *34*, 7406.
[17] F. Weigend, R. Ahlrichs, *Phys. Chem. Chem. Phys.* **2005**, *7*, 3297–3305.
[18] M. J. Frisch, G. W. Trucks, H. B. Schlegel, G. E. Scuseria, M. A. Robb, J. R. Cheeseman, J. A. Montgomery Jr, T. Vreven, K. N. Kudin, J. C. Burant, J. M. Millam, S. S. Iyengar, J. Tomasi, V. Barone, B. Mennucci, M. Cossi, G. Scalmani, N. Rega, G. A. Petersson, H. Nakatsuji, M. Hada, M. Ehara, K. Toyota, R. Fukuda, J. Hasegawa, M. Ishida, T. Nakajima, Y. Honda, O. Kitao, H. Nakai, M. Klene, X. Li, J. E. Knox, H. P. Hratchian, J. B. Cross, C. Adamo, J. Jaramillo, R. Gomperts, R. E. Stratmann, O. Yazyev, A. J. Austin, R. Cammi, C. Pomelli, J. W. Ochterski, P. Y. Ayala, K. Morokuma, G. A. Voth, P. Salvador, J. J. Dannenberg, V. G. Zakrzewski, S. Dapprich, A. D. Daniels, M. C. Strain, O. Farkas, D. K. Malick, A. D. Rabuck, K. Raghavachari, J. B. Foresman, J. V. Ortiz, Q. Cui, A. G. Baboul, S. Clifford, J. Cioslowski, B. B. Stefanov, G. Liu, A. Liashenko, P. Piskorz, I. Komaromi, R. L. Martin, D. J. Fox, T. Keith, M. A. Al-Laham, C. Y. Peng, A. Nanayakkara, M. Challacombe, P. M. W. Gill, B. Johnson, W. Chen, M. W. Wong, C. Gonzalez, J. A. Pople, *Gaussian 03*, Revision C.01, Gaussian, Inc., Wallingford, CT, **2004**.
[19] K. A. Peterson, D. Figgen, E. Goll, H. Stoll, M. Dolg, *J. Chem. Phys.* **2003**, *119*, 11113.
[20] D. G. Gorenski, *Phosphorus-31 NMR, Principles and Applications*, Academic Press, New York, **1984**.

Received: January 24, 2007
Published Online: May 8, 2007

 © 2007 Wiley-VCH Verlag GmbH & Co. KGaA, Weinheim